Pergamon

Int. J. Solids Structures Vol. 34, No. 9, pp. 1105–1122, 1997

0020-7683/97 $17.00 + .00

PII: S0020-7683(96)00067-4

CREEP RUPTURE OF POLYMERS–A STATISTICAL MODEL

MILENA VUJOSEVIC and DUSAN KRAJCINOVIC
Department of Mechanical and Aerospace Engineering, Arizona State University
Tempe Az 85287-6106, U.S.A.

(*Received* 25 *June* 1995; *in revised form* 15 *April* 1996)

Abstract—The paper focuses on the micromechanical origins and mechanisms of creep failure of epoxy-resins. Microstructure of the material is modeled by a 2D lattice. The probabilistic nature of the creep deformation process is based on the kinetic theory of rupture. The macroscopic manifestation of the process: evolution of strain, degradation of stiffness and endurance are defined in terms of the morphology of the microstructure and processes at the microlevel. © 1997 Elsevier Science Ltd. All rights reserved.

1. INTRODUCTION

A material subjected to stress levels which are well below its mechanical strength and high temperatures undergoes a time dependent deformation known as creep. The time to creep rupture is found to be proportional to the stress sign and magnitude, temperature and microstructure. The inquiry into the process of creep rupture has been motivated, in the last few decades, by the needs of the power generation industry, design of more powerful engines and turbines for aircrafts and automobiles, etc.. A variety of empirical, phenomenological (Hult, 1966, Rabotnov, 1969) and micromechanical (Riedel, 1987, Cocks and Leckie, 1987) models have been proposed in the past to predict the type of response and the time to creep failure as a function of temperature and applied stress (which is typically assumed to be constant for the duration of the deformation process). Most of these models are deterministic and based on the premise that the influence of the temperature can be introduced through the constitutive properties. A different viewpoint was taken by the material scientists and physicists (Regel' *et al.*, 1974, Poirier, 1985) who treat the temperature as a basic stimulus which enhances the mobility of atoms and increases the probability of dislocation motion and rupture of atomic bonds in the material. The competition between the rate of dislocation motion and the rate of the bond rupture determines the degree of brittleness in a particular material under specific circumstances.

Thermoset polymers are increasingly used in engineering applications. The relative ease of manufacturing light-weight components of complex shapes and the wide range of available physical properties makes these materials very attractive for industrial use. Thermoset resins are often employed in neat form, but find their principle application as matrix materials for composites. A high degree of cross-linking provides thermosets with rigidity and causes them to behave in a brittle manner. The brittle behavior remains at elevated temperatures, when the principle mechanism of deformation is microcracking. These issues motivate the high temperature application of thermosetting polymers, rendering creep rupture analysis especially important.

The objective of this study is to consider the creep deformation as being a thermally activated process and take into consideration the stochastic nature of thermal fluctuations and properties of the microstructure. The study is focused on the brittle deformation of thermoset polymers which is attributable to the sequential rupture of molecular chains. The microstructural morphology of epoxy resins (Mijovic and Tsay, 1981) emphasizes dense nodules interconnected by lower density material formed by crosslinked polymer chains and can be modeled by a central-force lattice (three dimensional truss—see Krajcinovic and Mallick, 1994, 1995). All lattice properties can be determined from the atomic

and molecular properties of the resin. However, since the inter-nodular distance is very small ($\approx 0.5 \times 10^{-8}$ m) a model of a typical engineering specimen would require a lattice with far too many elements to be useful in application. Hence, it is important to explore the effect of the lattice size on the macro response and time to rupture.

In addition to the lattice model which can account for the interaction of defects and the effects of stress concentration, the study also formulates a mean field model, and examines the validity of the first order effective medium approximations.

2. ANALYTICAL MODEL AND THE KINETIC CRITERIA OF RUPTURE

The analysis focuses on a prismatic specimen subjected to the uniform tensile stresses of constant magnitude and temperature close to the glass transition temperature T_g of a thermoset. The specimen is, for the case of plane strain condition, approximated by a two-dimensional, triangular central-force lattice of perfect geometry (Fig. 1.a). The nearest neighbor nodes are connected by the links of identical stiffness k, identical strength f_c, identical length l and identical activation energy U_0. The force-displacement relation of the link is linear up to failure. The spring stiffness k is related to the elastic modulus E of the resin by the relation $k = (8/5\sqrt{3})E$ per unit thickness (Monette and Anderson, 1994). The Poisson's ratio of the lattice $\nu = 1/3$ is independent of the spring stiffness k. However, the strength in two directions is not the same (Monette and Anderson, 1994).

The morphology of epoxy lattices is neither topologically nor geometrically perfect. it is also not two-dimensional. However, the primary objective of this study is to establish micromechanically based relations for the evolution of the strain and damage in time. In view of the assumptions used to simplify the morphology of the resin microstructure the presented results are qualitative in nature. More specifically, in the case of temperature

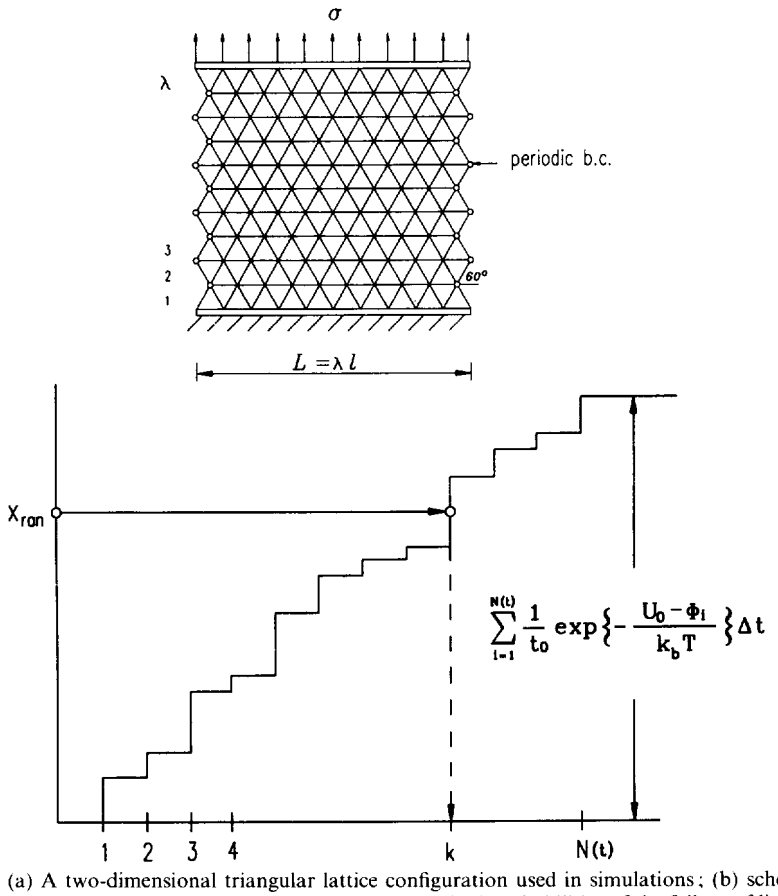

Fig. 1. (a) A two-dimensional triangular lattice configuration used in simulations; (b) schematic showing the random process of link rupture. The individual probabilities of the failure of links are represented as flights of the staircase. Link k is ruptured when the random number x_{ran} exceeds the cumulative height of the k^{th} staircase.

driven damage evolution the assumption of perfect geometry should not have any effect on the corresponding mode of failure (elastic percolation) since the percolation threshold depends entirely on the topology (coordination factor) of the lattice. However, the same approximation can have a quantitative effect on the accuracy of the result if the damage evolution is driven by stresses (induced by mechanical load) which depend on the geometry.

The stochastic nature of the problem is introduced through the kinetic rupture criterion based on the absolute reaction-rate theory of Eyring (1936). Within the framework of the reaction-rate theory the bonds (links) of a lattice are viewed "as coupled oscillators in a state of thermal vibration" (Termonia *et al.*, 1985). The bond rupture is treated as a random process which is activated by the spatially and temporally random thermal fluctuations. The probability that the i-th link will rupture during the time interval Δt is proportional to the rate of the link rupture R_f (Krajcinovic and Mallick, 1994, 1995)

$$p_f^i = R_f \Delta t = \frac{1}{t_0} \exp\left(- \frac{U(f_i)}{k_b T} \right) \Delta t = \frac{1}{t_0} \exp\left(- \frac{U_0 - \tilde{\Phi}_i(t)}{k_b T} \right) \Delta t \tag{1}$$

where $U(f_i)$ is the apparent activation energy, $U_0 = 2 \times 10^{-19}$ J is the activation energy of an unstressed bond or the height of the energy barrier in the stress-free state, $t_0 = 10^{-12}$ s the mean period of atomic thermal vibrations, $k_b = 1.381 \times 10^{-23}$ J/molK (Boltzmann's constant) and T the absolute temperature in degrees Kelvin. The term $\tilde{\Phi}_i(t) = \Phi_i \text{sign}(f_i)$ is related to the elastic energy stored in the i-th link $\Phi_i(t) = f_i^2/2k$, where the link force $f_i(t)$ depends on the state of the lattice. The effect of the elastic energy $\Phi_i(t)$ on the energy barrier is taken with a positive sign when the force in the link is tensile and with a negative sign when the force is compressive. In crystals the constant U_0 "fits well to the energy of sublimations....(and)... is equal to the binding energy of atoms" (Zurkov, 1965). Similar conclusions can be reached by consulting voluminous data for metals, glasses and polymers of Regel' *et al.*, (1974).

On the atomic scale (Bueche, 1955, and Regel' *et al.*, 1974, Ch. III.2) the activation energy is equal to $U(f_i) = U_0 - \tilde{\Phi}(f_i)$ where $\tilde{\Phi}(f_i)$ is the elastic energy stored within the link. On the macroscopic scale the activation energy for thermoplastics is often written as a linear function of force as $U(f_i) = U_0 - \gamma f_i$ where γ is the activation volume (Termonia *et al.*, 1985). Indeed, Termonia *et al.* (1985) preferred the latter expression on the basis of a better fit for the case of polyethylene fibers. However, the scatter in measurements for the activation volume (0.7–3.0 for zinc, 2.0–9.0 for aluminum, 0.29–0.43 kcal mm^2/mole kg for capron—Table II in Ch. II.9 from Regel' *et al.*, 1974) does not render the best fit criterion entirely convincing. For example, Krausz and Krausz (1988) use the energy release rate for $\tilde{\Phi}(f_i)$ for the propagation of the macroscopic crack.

One of the reasons for the disagreement in selection of the parameter $\tilde{\Phi}(f_i)$ is the entropic nature of the elasticity of a polymer chain (Mears, 1965), i.e. a chain can be stretched by changing its conformation without any storage of energy. However, the nodules (aggregates) in a thermoset are interconnected by a network of crosslinked polymer chains. The stiffness of a crosslinked network depends on the number of polymer chains, distance between the aggregates and temperature. Furthermore, the elasticity of a crosslinked network in thermosets is dominated by the energy stored in the links rather than conformation, since, in the limit of small strains (Perepechko, 1981) the force in the link (network) is linearly proportional to the link elongation. In summary, since the objective of this work is to examine the creep deformation of a thermoset polymer (modeled by a system of aggregates linked together by crosslinked networks) it seems that the parameter $\tilde{\Phi}(f_i)$ should be, on observed scale, selected in form of the elastic energy stored in the network (as suggested originally by Bueche, 1955).

The link failure probabilities (1) are constant as long as the link forces f_i remain constant. Hence the time interval must be selected such that only a single link ruptures as $t \to t + \Delta t$. Thus, the average time needed for the rupture of a link is from (1) equal to

$$\Delta t = t_0 \left[\sum_{i=1}^{N(t)} \exp\left(- \frac{U_0 - \tilde{\Phi}_i(t)}{k_b T} \right) \right]^{-1} \tag{2}$$

The summation in (2) extends over all extant links $N(t)$.

The exact sequence of link ruptures is determined by the Monte Carlo lottery (Dobrodumov and El'yashevich, 1973, Termonia *et al.*, 1985, 1987, 1988, 1989). At each time interval (2) the forces in each link are determined by using simple algorithms for the elastic central-force lattices (trusses). The probabilities (1) are computed and arranged into the cumulant function shown in Fig. 1.b. The link that will rupture during the time period $(t,t+\Delta t)$ is identified by the point in which a horizontal line drawn from the randomly selected point on the ordinate intersects the cumulant function. The lattice elongation, current stiffness and the fraction of ruptured bonds is computed and recorded at each time interval. The computations are terminated when an infinite (spanning) cluster of defects emerges and reduces the lattice stiffness to zero.

The relative effects of temperature and stress on final rupture are reflected in the link rupture probabilities (1). At relatively large stresses the apparent activation energy $U(f_i) = U_0 - \tilde{\Phi}_i(t)$ of the links near the defect (stress concentrations near ruptured bonds) are much lower than the activation energy of links far away from the defect. Hence, the probability that the links near the defect will fail first is substantial. As the defect (cluster of ruptured links) grows so does the probability that the link at its tip will rupture next. The specimen rupture is in this case of the brittle (cleavage) mode which emphasizes propagation of a single crack. At very small tractions the apparent activation energies $U(f_i)$ and rupture probabilities (1) are almost identical for all links. As a result the damage will be randomly distributed over the entire lattice. The failure of the specimen will in this case occur at a substantial damage density distributed over the entire specimen volume.

3. LATTICE SIMULATIONS—RESULTS

The model which is considered consists of $\lambda \times \lambda$ two-dimensional triangular network of springs (Fig. 1.a). The non-dimensional lattice size is related to the actual geometrical lattice size by the relationship $\lambda = L/l$ where l is the link length. The link size l is also the resolution length of the model which coincides with the characteristic length of the microstructure (the inter-nodular distance). The boundary conditions of the lattice are prescribed as follows. The bottom row of the lattice is fixed. The top row of nodes is subjected to a uniform tensile stress $\sigma = const.$ In the lateral direction, periodic boundary conditions are imposed to avoid shape effects. Simulations are performed over many physical realizations, for different lattice sizes and different magnitudes of applied stress. The average temperature $T = 0.75T_g$ is kept constant for all simulations.

The kinematics of lattice deformation is defined by the lattice elongation and a damage parameter. For example, the fraction of ruptured links or the reduction of the lattice stiffness (Hansen *et al.*, 1989, Krajcinovic and Basista, 1991, etc.) can be selected to measure the damage on the scale of the lattice. The most important parameter for design is the time of rupture which may or may not depend on the accumulated damage, lattice size, stress concentrations, defect size distribution, etc.

3.1. *Fraction of ruptured bonds at creep failure*

On the atomic scale, damage is defined by the probability that a particular bond is broken. On the macroscopic scale the damage can be measured only indirectly by the effect it has on the macro response of the specimen (Krajcinovic and Mastilovic, 1995). The most important aspect of damage modeling is to single out the damage measure which is readily identifiable, measurable in tests, robust with respect to the details of experimental observations and independent of the specimen size. The first task is to establish the relationship between the fraction of ruptured bonds and the effective (lattice) stiffness. Since the horizontal bonds do not contribute to the stiffness of the lattice in the direction of the applied loads only the fraction of the ruptured diagonals are of interest.

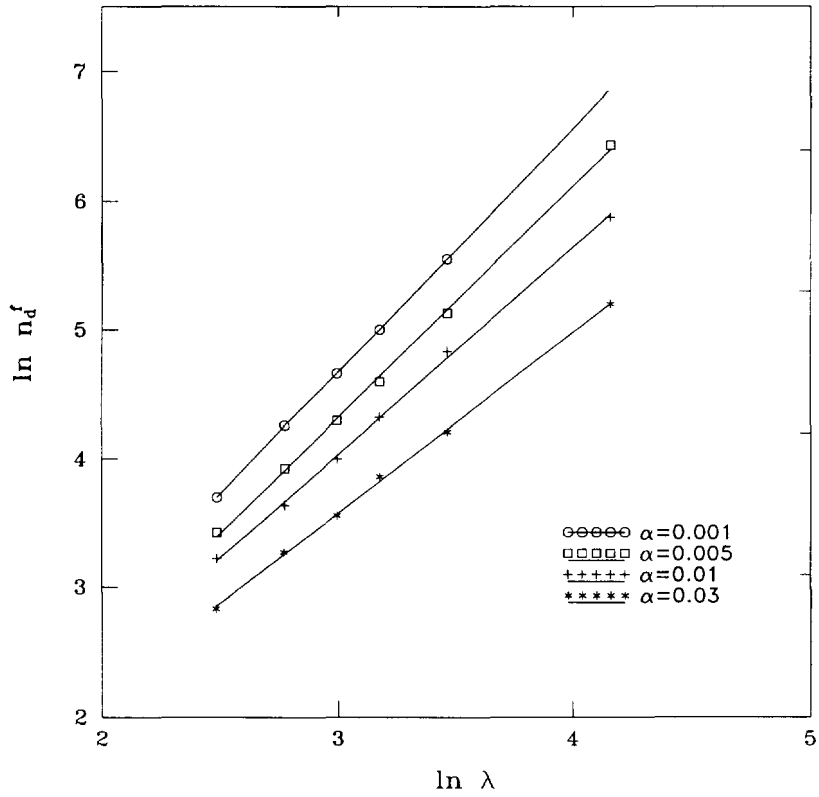

Fig. 2. The number of ruptured diagonals n_d^f at system failure vs lattice size λ for various α. The slopes γ of the straight lines for $\alpha = 0.001$, 0.005, 0.01, and 0.03 are 1.88, 1.80, 1.61, and 1.40, respectively.

The simulations performed in this study (Fig. 2) indicate that the fraction of the broken diagonals at failure scales with the specimen size λ as

$$q_d^f = \frac{n_d^f}{N_d} \propto \lambda^{\gamma}, \tag{3}$$

where n_d^f is the number of ruptured diagonals at lattice failure, and $N_d = 2\lambda^2$ the initial number of diagonals.

The ratio

$$\alpha = \frac{\Phi_t(0)}{U_0} = \frac{\Phi_0}{U_0} \tag{4}$$

defines the fractional reduction of the activation energy which is attributable to the externally applied mechanical loads. The subscript "0" denotes reference to the pristine (undamaged) state and C_0 the axial stiffness of the undamaged lattice.

The dependence of the scaling exponent on the load parameter α is displayed on Fig. 2. At minuscule load intensities, i.e., as $\alpha \to 0^+$ the scaling exponent $\gamma \to 2^-$ since the geometry of the diluted lattice is self-similar at the percolation threshold. In the absence of mechanical stresses the bond rupture sequence is perfectly random and the damage evolves by defect nucleation only. A randomly diluted lattice fails in the percolation mode after accumulation of a substantial density of distributed damage. As the load parameter α is increased the exponent γ in the expression (3) tends to unity. This is also consistent with the fact that the failure at large stresses occurs when a single crack, formed by 2λ ruptured diagonals, traverses the specimen. The absence of distributed damage minimizes the specimen fracture energy. A similar scaling behaviour was reported by Hansen *et al.*, (1990), and Curtin and Scher (1991), for a different link rupture criterion.

The density of ruptured bonds at failure is size independent only when the lattice dilution is perfectly random, i.e., when $\alpha \to 0^+$. In all other cases the damage density at the lattice failure decreases with the increase of the specimen size.

3.2. *Lattice stiffness*

The total number and density of ruptured links (i.e., damage in the specimen) are dependent on the specimen size λ (Fig. 2). Hence, neither the total number of ruptured bonds nor the density provide a viable measure of damage at failure. The next task is to ascertain whether the lattice stiffness is size independent.

A random dilution of stress-free central-force lattices ($\alpha = 0$) has been studied within the framework of the percolation theory by many authors (Feng and Sen, 1984, Lemieux *et al.*, 1985, Sahimi and Goddard, 1986, Beale and Srolovitz, 1988, etc.). The mean field estimate of the lattice stiffness is

$$\frac{C}{C_0} = \frac{p - p_c}{1 - p_c} = \frac{zp - 4}{z - 4} \tag{5}$$

where p is the fraction of surviving links at time t, p_c the critical fraction of surviving links at the percolation threshold, and z the coordination number (number of bonds intersecting at a node). The mean field estimate of the critical fraction of surviving links in a triangular lattice ($z = 6$) at the percolation threshold ($C = 0$) is, from (5), $p_c = 2/3$. This result is within numerical scatter equal to the value $p_c \approx 0.63$ determined by the simulations of Beale and Srolovitz (1988) and very close to the value determined experimentally by Sieradzki and Li (1986). As shown by Feng and Sen (1984) and Beale and Srolovitz (1988) the linear dependence of the lattice stiffness on the number of ruptured bonds persists over a surprisingly large range ($1 \geqslant C/C_0 \geqslant 0.1$).

The computer simulations performed in this study demonstrate identical trends for the small values of the load parameter α (Fig. 3). The dependence of the lattice stiffness on the

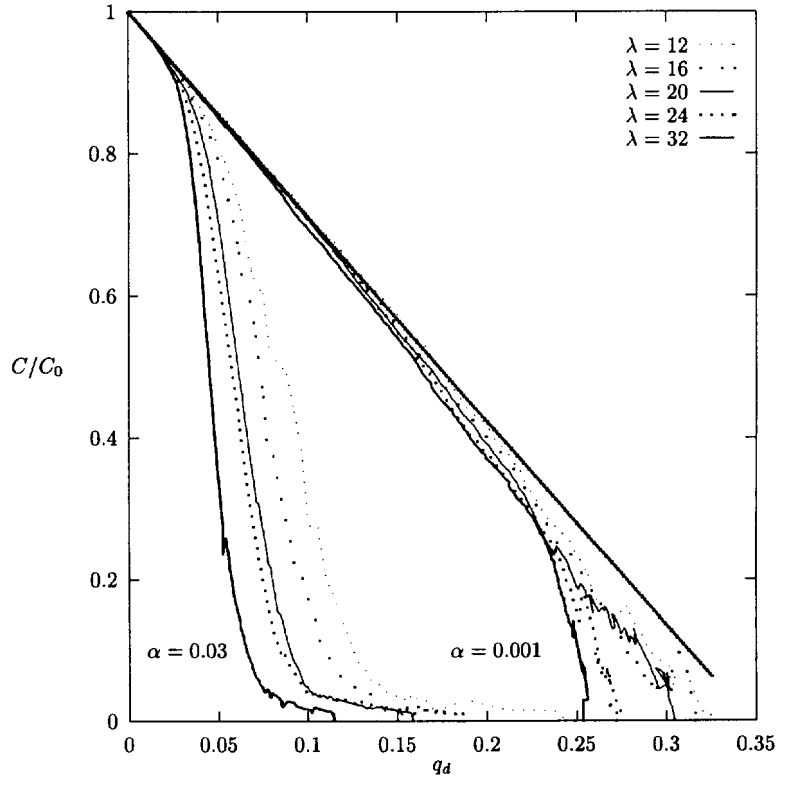

Fig. 3. Reduction of the lattice stiffness C/C_0 vs fraction of broken diagonals q_d in the course of simulation for $\alpha = 0.001$ (right set of curves) and $\alpha = 0.03$ (left set of curves) and different lattice sizes. The straight line $C/C_0 = 1 - q_d/q_c$, ($q_c = 0.3473$), represent the percolation type process ($\alpha = 0$).

fraction of ruptured diagonals is displayed in Fig. 3 taking α and lattice size λ as parameters. The cross-over from the thermally activated, defect nucleation dominated damage evolution process ($\alpha \to 0^+$), to stress driven, defect growth dominated damage accumulation ($\alpha = 0.03$), is apparent from the two sets of curves in Fig. 3. A rapid loss of lattice stiffness at modest accumulation of damage is typical of the stress driven propagation of defects. Failure takes place at an almost imperceptible loss of stiffness $C/C_0 \approx 0.95$. Lattice failure of a thermally activated and driven process of defect nucleation occurs at large defect density and after an observable loss of stiffness. The brittle character of the failure is amplified when the lattice size is increased.

3.3. *Evolution of the strain with time*

Phenomenologically, creep deformation is often divided into three phases (Fig. 4). The strain rate during the first or *primary* creep phase is very high. The deformation is at small stress levels, for all practical purposes, elastic and instantaneous. The strain rate during the *secondary* phase is practically constant. The loss of stiffness is, therefore, a linear function of time. By inference, the damage evolution during the secondary (stationary) phase, is attributable primarily to the nucleation of defects which are scattered over the entire volume of the specimen. The specimen microstructure is statistically homogeneous (Fig. 5.a) and the response is of the mean field type. As long as the probabilities of the interaction of neighboring defects is small, the probabilities of link rupture (1) are practically identical. Stress concentrations play a modest role in the damage evolution process. The effect of the stress concentrations on the stiffness and the response becomes more pronounced as the defect density increases. The probability of interaction of closely spaced defects increases leading to the formation of a large defect. The formation and propagation of large cracks or defect clusters in the *tertiary* creep phase have a dramatic effect on the rate of the stiffness degradation and the increase of the strain rate. The rupture probabilities of links near the tip of a large crack are so large that the process of nucleation crosses over to the process dominated by the growth of a single crack (Figs 5a–d). The ensuing damage evolution is

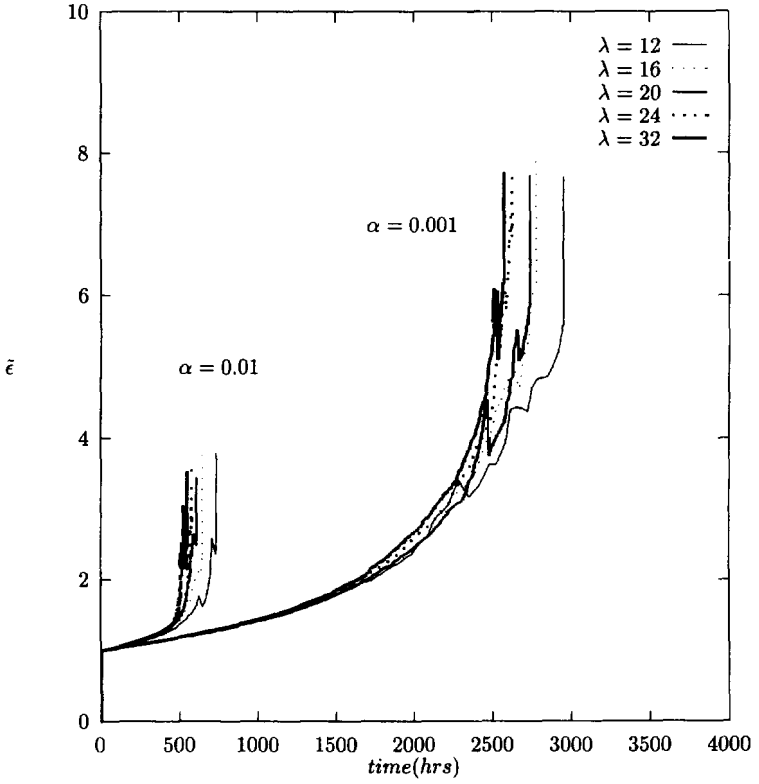

Fig. 4. Evolution of creep strain $\bar{\varepsilon}$ with time for different lattice sizes and two values of the load parameter: $\alpha = 0.001$—right set of curves and $\alpha = 0.01$—left set of curves).

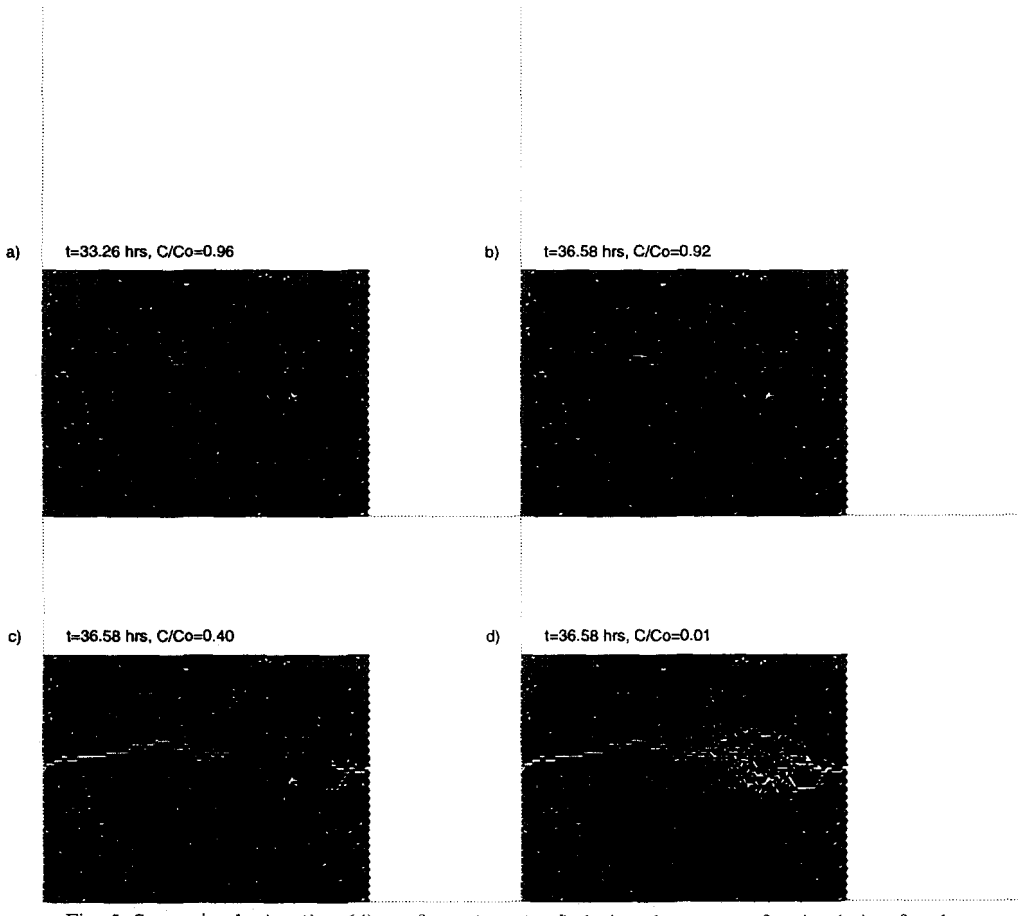

Fig. 5. Successive lattice ($\lambda = 64$) configurations (a–d) during the course of a simulation for the load parameter $\alpha = 0.03$. Indicated are the corresponding times and reduction of stiffness.

dominated by stress concentration driven defect growth. The smooth transition between successive phases is referred to as the cross-over regime during which the balance between the competing mechanisms of damage evolution changes. This part of the process, characterized by the gradual increase in strain rate and modest size dependence, reflects the growing effect of the cooperative (or defect interaction) phenomena. For large values of the load parameter α, this phase of the process is very short (Fig. 4), and the process of the defect nucleation is directly followed by the process of single crack propagation (Curtin and Scher, 1991).

A variety of phenomenological creep models, based on different rheological models and different relations between stresses and strain rates, are available in the literature (Hult, 1966, Rabotnov, 1974, etc.). According to the Tobolsky and Eyring (1943) model, which is compatible with the simulations presented here, the strain is related to the elapsed time t by

$$\varepsilon = A_1 - A_2 \ln(t_f - t) \tag{6}$$

where t_f is time to rupture. Constants A_1 and A_2 can be determined in terms of observable and measurable parameters from

$$\tilde{\varepsilon}(t)|_{t=0} = \left.\frac{\varepsilon(t)}{\varepsilon_e}\right|_{t=0} = 1 \quad \text{and} \quad \left.\frac{\mathrm{d}\tilde{\varepsilon}}{\mathrm{d}t}\right|_{t=0} = w \tag{7}$$

where ε_e is the instantaneous, elastic strain and w a parameter which depends on the material microstructure and the temperature.

In the case of brittle deformation the nonlinearity of the stress-strain relations can be traced to the degradation of the stiffness, i.e., to the accumulated damage (Kachanov, 1958). Hence, the normalized strain is

$$\tilde{\varepsilon}(t) = \frac{1}{1-D(t)} \tag{8}$$

where the damage parameter

$$D(t) = \frac{C_0 - C(t)}{C_0} \tag{9}$$

is defined as the fractional loss of lattice stiffness (Krajcinovic and Basista, 1991). At very small damage densities (early phase of the deformation process) the damage accumulation is a linear function of the ruptured bonds (Fig. 3), i.e., $D(t) = q(t)/q_c$, where $q = 1-p$ and $q_c = 1-p_c = 0.3473$ is the fraction of missing links at the rigidity elastic percolation threshold for a central-force triangular lattice (Stauffer and Aharony, 1992). The corresponding strain rate is

$$\left.\frac{\mathrm{d}\tilde{\varepsilon}}{\mathrm{d}t}\right|_{t\to 0^+} = \frac{1}{q_c}\left(1-\frac{q}{q_c}\right)^{-2}\left.\frac{\mathrm{d}q}{\mathrm{d}t}\right|_{t\to 0^+}. \tag{10}$$

The rate at which the bonds rupture is, from (1) and (2),

$$\frac{\mathrm{d}q}{\mathrm{d}t} = \frac{1}{N}\sum_{i=1}^{N(t)}\frac{1}{t_0}\exp\left(-\frac{U_0-\tilde{\Phi}_i(t)}{k_bT}\right). \tag{11}$$

Hence,

$$\frac{\mathrm{d}q}{\mathrm{d}t} = \frac{1}{t_0}\exp\left[-\frac{U_0(1-\alpha)}{k_bT}\right] \quad \text{at } t = 0. \tag{12}$$

The approximate expressions for the strain and the stiffness are then

$$\tilde{\varepsilon}(t) = 1 + \frac{1}{q_c t_0}\exp\left[-\frac{U_0(1-\alpha)}{k_bT}\right] t_f \ln\frac{t_f}{t_f - t} \tag{13}$$

and

$$\frac{C(t)}{C_0} = \left\{1 + \frac{1}{q_c t_0}\exp\left[-\frac{U_0(1-\alpha)}{k_bT}\right] t_f \ln\frac{t_f}{t_f - t}\right\}^{-1}. \tag{14}$$

The results of the numerical simulations are compared to the approximate expressions (13) and (14) in Fig. 6 for the load parameter $\alpha = 0.01$ and five different lattices sizes λ. In view of the random character of the deformation process, the accuracy with which (13) and (14) fit the simulation data is remarkable.

It is important to notice that the proposed model includes only a single parameter t_f. Hence, the accuracy of the model depends on the accuracy of the estimate of t_f. Moreover, the response and the effective stiffness are size independent if and only if t_f is size independent.

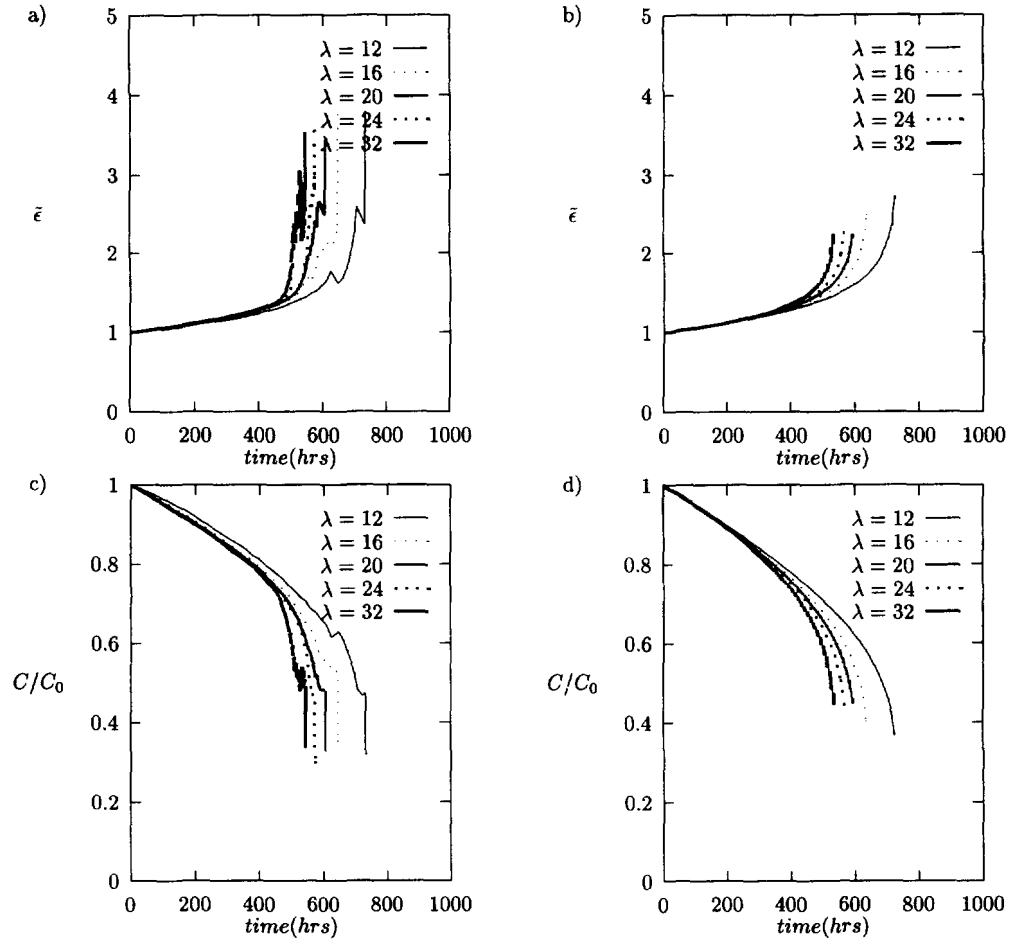

Fig. 6. Comparison between the simulation (*a* and *c*) and analytical (*b* and *d*) results for evolution of creep strain $\bar{\varepsilon}$ with time and reduction of the specimen stiffness C/C_0 with time. Load parameter $\alpha = 0.01$.

3.4. *Time to creep failure*

The time to creep failure is the most important parameter, which depends on the constitutive properties (through the parameters U_0, t_0), topology of the microstructure (through the percolation threshold $p_c = 1 - q_c$), specimen size λ, temperature T and the applied loads (load parameter α). The rupture is defined as a state at which the lattice stiffness C vanishes, i.e., by $C(t) \to 0$ as $t \to t_f$. The time to failure is determined from the computer simulations as

$$t_f = \sum_{n=0}^{n_f} \Delta t_n \tag{15}$$

where n_f is the number of ruptured bonds at lattice failure while Δt_n is defined by (2).

The simulation results, plotted in Fig. 7, indicate the exponential dependence of the time to rupture on the applied tensile stresses

$$\ln t_f = c - a(\lambda)\sqrt{\alpha} \tag{16}$$

which is in agreement with the experimentally observed trends (Regel' *et al.*, 1974).

The parameter c defines the time of rupture of a stress-free specimen. For $\Phi \equiv 0$, it follows from (2) that

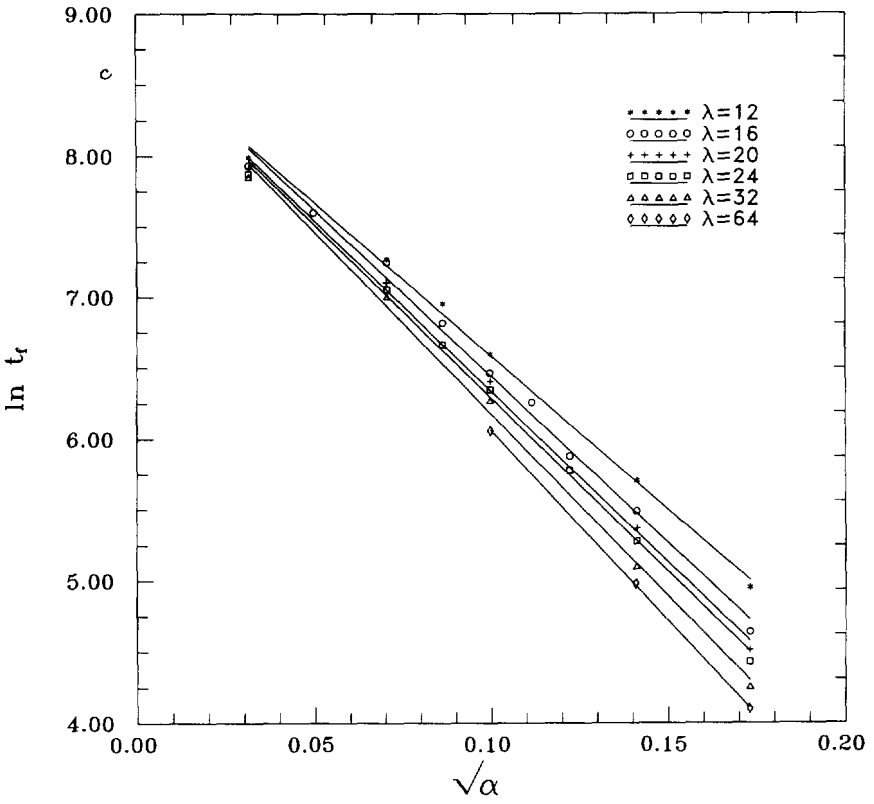

Fig. 7. Variation of the time to failure t_f with load parameter α for different lattice sizes.

$$t_f(\Phi \equiv 0) = t_0 \exp\left(\frac{U_0}{k_b T}\right) \sum_{n=0}^{q_c N} \frac{1}{N-n} = \ln \frac{1}{1-q_c} t_0 \exp\left(\frac{U_0}{k_b T}\right) \tag{17}$$

where q_cN is the number of ruptured links at the percolation threshold. The expression for the time to rupture can be rewritten as

$$t_f = \ln\left(\frac{1}{1-q_c}\right) t_0 \exp\left(\frac{U_0}{k_b T}\right) \exp\left[-a(\lambda)\sqrt{\alpha}\right] \tag{18}$$

the parameter $a(\lambda)$ was evaluated from the simulations and Fig. 8 as

$$a(\lambda) = 27.59 - 69.60 \frac{1}{\lambda}. \tag{19}$$

The dependence of the time to creep rupture on the specimen size, defined by (18), is displayed in Fig. 9. Since the internodular distance (links length) in polymers is only $l \approx 0.5 \times 10^{-8}$ m the specimen size influences the time to creep rupture only in very small specimens. For example, if $\alpha = 0.03$ the time to rupture will be size dependent only for specimens shorter than $L < 100\, l = 0.5\ \mu$m. The size dependence refers, in this case, to the specimen length in the direction of the applied loads since the specimen width was rendered infinitely long by the imposition of the periodic boundary conditions along the vertical sides.

In the considered problem, the duration of the tertiary creep phase is very small compared to the secondary creep phase. At rather modest stresses and large temperatures most of the specimen lifetime is consumed by the nucleation of microcrack densities needed to form a cluster which is large enough to start growing at a rapid rate. There is a weak effect of size on crack nucleation (Bolotin, 1989) and this explains the fact that the time to rupture is almost entirely size independent. It is important to note that this study considers

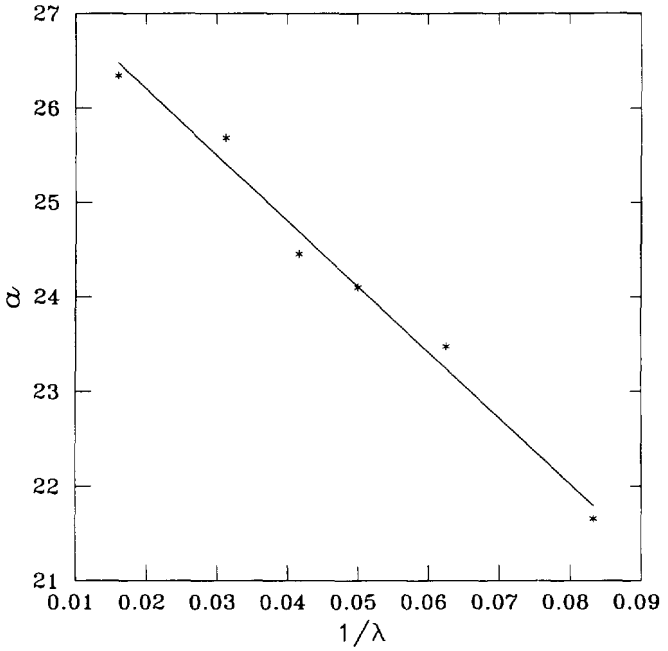

Fig. 8. The dependence of the parameter $a(\lambda)$ on the lattice size λ.

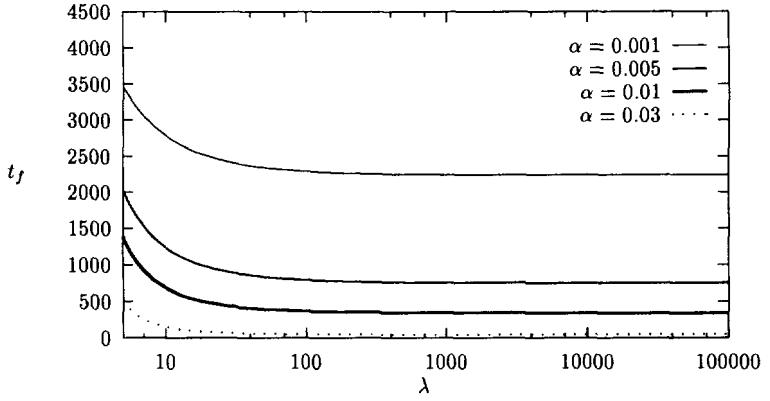

Fig. 9. The size dependence of the time to failure t_f for different values of the load parameter α.

the creep rupture of specimens which are initially not damaged. If the specimens were pre-damaged and subjected to large tensile tractions their strength would exhibit significant size dependence (Duxbury, 1994).

The cumulative probability distribution function of the time to failure $F(t_f)$ is determined from the simulations for different lattice sizes (Fig. 10). As expected, the scatter of the results decreases with the increase of lattice size. It is of interest to explore if $F(t_f)$ can be cast into some of the familiar form of probability distributions. The survival probability depends on the probability of finding a large crack in the specimen. Moreover, the size of the stress induced defects is distributed according to Weibull's law (Curtin and Scher, 1992). Since lattice rupture depends on the largest defect it seems reasonable to assume that the cumulative probability of the time to creep rupture can be written in the form of the Weibull distribution

$$F(t_f) = 1 - \exp\left[-\left(\frac{t_f}{t^*}\right)^m\right] \tag{20}$$

as anticipated by Bolotin (1989). The Weibull probability plots for different sizes of specimen λ (and fixed load parameter $\alpha = 0.01$) and different applied stresses (and fixed lattice

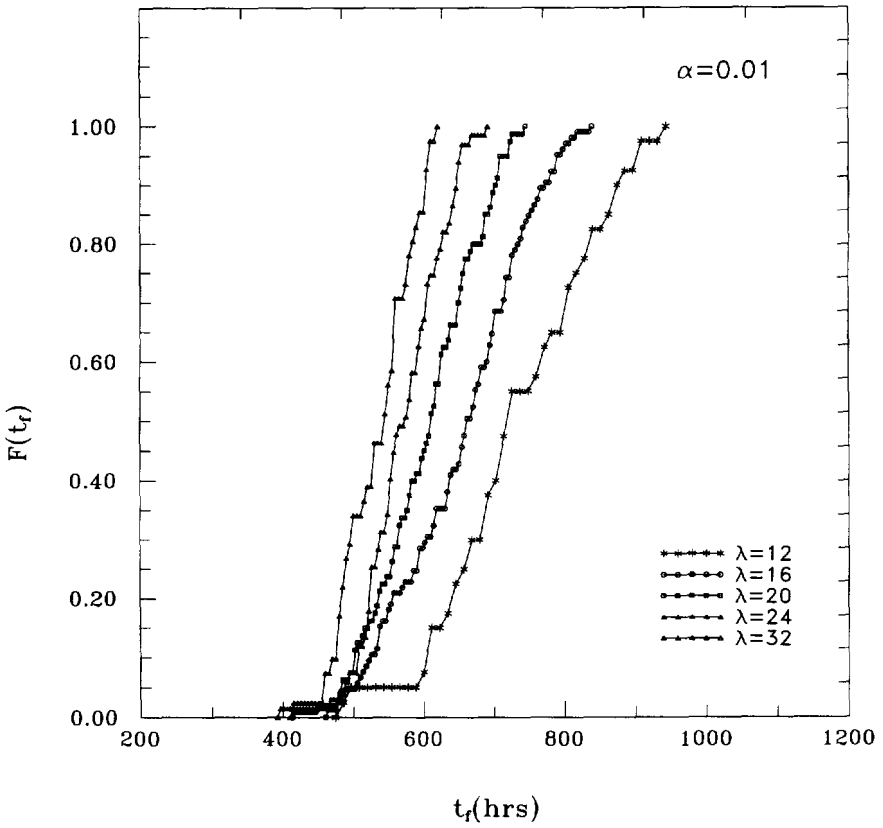

Fig. 10. The cumulative probability distributions of time to failure for different lattice sizes and $\alpha = 0.01$.

size $\lambda = 16$) are displayed in Fig. 11. The justification for the Weibull's distribution of defects is supported by the linearity of the graphs in Fig. 11. The shape factor $m = m(\lambda)$ is very weakly size dependent while the scale factor $t^* = t^*(\Phi)$ is a function of the applied tensile stresses.

4. MEAN FIELD MODEL

The stiffness of a specimen subjected to creep deformation is, at least initially, dominated by the nucleation of microcracks. During this early phase the damage is randomly distributed over the entire specimen volume. The overall response is of the mean field type.

The mean field models (Nemat-Nasser and Hori, 1993) are based on the assumption that each defect is subjected to an equal strain computed from the applied stresses and the effective stiffness. Hence, the exact position of each defect is irrelevant and the direct interaction of adjacent defects is neglected. The mean field and effective continua models are supposed to be valid at modest densities of uniformly distributed defects, i.e. when the specimen is statistically homogeneous. Since the mean field models lead to simple estimates of macro parameters, it is of obvious interest to ascertain the accuracy of these estimates.

The parallel bar model (Krajcinovic *et al.*, 1993) represents a discrete analog of the first order mean field models. In the loose bundle parallel bar approximation a specimen subjected to uniaxial tension is modeled by an ensemble of N links. All links are assumed to have equal stiffness $k = C_0/N$ (where C_0 is the stiffness of the pristine specimen) and equal strength. The system is at each end provided by a rigid busbar which can move only in the direction of the applied force $F = const.$ (Fig. 12.a). Consequently, all extant links equally share in supporting the externally applied force and are subject to the identical elongation $u(N_t, t)$ (where $N_t = N - n$ is the number of extant links and n the number of ruptured links). The force carried by a link is

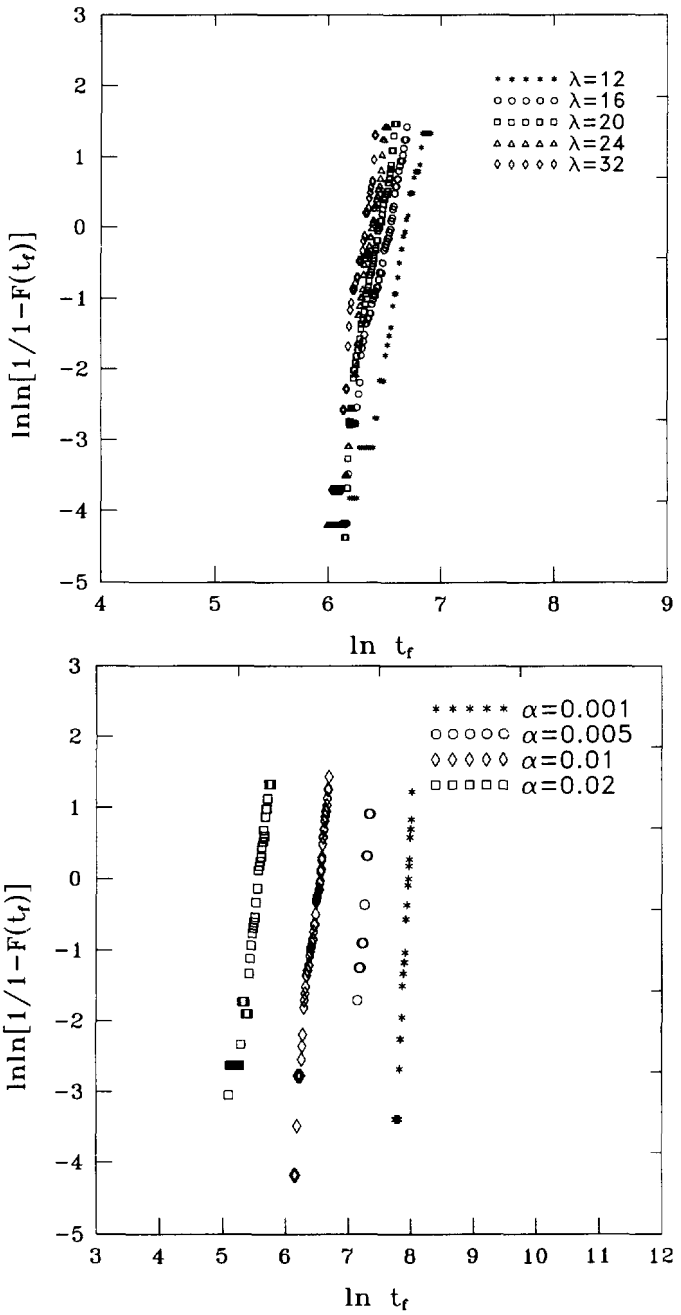

Fig. 11. The Weibull probability plots of the time to failure t_f: (a) for different sizes specimen (λ), load parameter $\alpha = 0.01$; (b) for different applied stress (α), lattice size $\lambda = 16$.

$$f(t) = \frac{F}{N-n(t)} = \frac{F}{N_t(t)} = \frac{F}{N[1-D(t)]} \tag{21}$$

where, from (9)

$$D(t) = \frac{n(t)}{N} = \frac{N-N_t(t)}{N} = 1-\frac{N_t(t)}{N} \tag{22}$$

is the damage parameter (Krajcinovic and Silva, 1982, Krajcinovic *et al.*, 1993).

The system elongation is

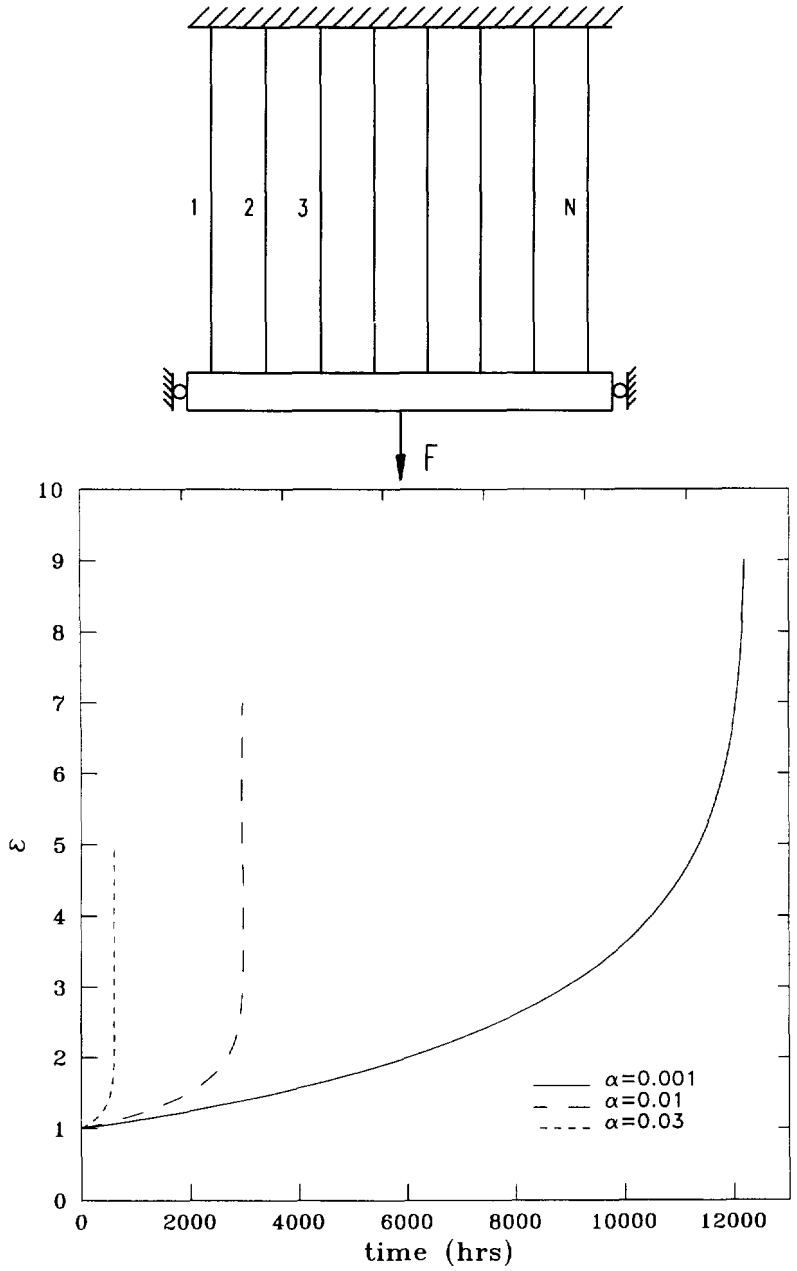

Fig. 12. (a) The parallel bar model; (b) evolution of creep strain with time.

$$u(t) = \frac{F}{C(t)} = \frac{F}{N_t(t)k} = \frac{F}{C_0[1-D(t)]}. \tag{23}$$

All extant links have an identical probability of rupture since they carry equal force f (21). The rate of link ruptures is, therefore,

$$R_f = \frac{1}{t_0}\exp\left\{-\frac{U_0}{k_bT}\left[1-\alpha\left(\frac{u(t)}{u_0}\right)^2\right]\right\} \tag{24}$$

where $u_0 = F/C_0$ is the elongation of the pristine system. The rate at which the link ruptures must be directly proportional to the number of surviving links and the rate of link ruptures. Moreover, in the mean field approximation this proportionality must be linear. Hence,

$$\frac{dN}{dt} = -R_f N_t. \tag{25}$$

The differential equation

$$dt = t_0 \exp\left(\frac{U_0}{k_b T}\right) \exp\left[-\frac{U_0}{k_b T}\alpha\left(\frac{1}{1-D}\right)^2\right]\frac{dD}{1-D} \tag{26}$$

can be readily derived by combining expressions (24) and (25). Subject to initial $D(t = 0) = 0$ and terminal condition $D(t = t_f) = D_{cr}$ the nonliner differential eqn (26) can be integrated as follows

$$t_f = t_0 \exp\left(\frac{U_0}{k_b T}\right)\int_0^{D_{cr}} \exp\left[-\frac{U_0}{k_b T}\alpha\left(\frac{1}{1-D}\right)^2\right]\frac{dD}{1-D}. \tag{27}$$

The integral in (27) can be written in the form of exponential integral functions

$$t_f = \frac{1}{2}\left\{E_i\left(\frac{\alpha U_0}{k_b T}\right) + E_i\left[-\frac{\alpha U_0}{k_b T}\left(\frac{1}{1-D_{cr}}\right)^2\right]\right\} t_0 \exp\left(\frac{U_0}{k_b T}\right). \tag{28}$$

the strain vs time curves for the parallel bar model exhibit the trends typical of creep deformation (Fig. 12.b). The dependence of the time to creep rupture (28) on the load parameter α is displayed in the graphs plotted in Fig. 12.b.

The difference between the parallel bar model and lattice models is that the former neglects the spatial correlations of defects. The spatial correlations is reflected in the topology of the system and the stress concentrations. For example, the fraction of ruptured links at system failure $q_c^{pbm} = 1$ for the parallel bar model and only $q_c^l = 0.35$ for the lattice model. Furthermore, the effect of stress concentration increases with the increase of damage and leads to an increase of strain rates in the tertiary creep phase. Both effects tend to decrease the duration of the second and third phase. Consequently, the mean field estimates of the time to creep rupture are upper bounds on the exact solution.

The difference in topology at the time of failure can be corrected by setting $D_{cr} = 0.35$. In that case, the discrepancy in the time to creep rupture: $t_f^{pbm}/t_f^l \approx 1.4$, 3.7 and 7.8 for $\alpha = 0.001$, 0.01 and 0.03, respectively, must be attributed to the spatial correlations. The mean field estimate becomes progressively worse as the stresses (and stress concentrations) are increased. Thus, even though the type of response is qualitatively similar, the mean field models are inherently incapable of a rigorous estimate of failure thresholds.

5. SUMMARY AND CONCLUSIONS

The proposed model for the creep deformation and failure of thermoset resins is based on the following hypotheses: (a) the macro response of the specimen is related to the morphology of the network formed by molecular chains, (b) the rupture of the molecular chains is a random process which is activated by the temperature and the applied stress, and (c) the damage evolution is an "annealing" process during which the state can be changed by the mobility of thermally stimulated conformation changes of molecular chains.

The macro response in the secondary creep phase is attributed to the thermally activated nucleation of defects formed by ruptured bonds. Local stress concentrations become the primary cause of the damage evolution dominated by the growth of the existing microcracks (tertiary creep) at larger damage accumulations and larger defects. The specimen ruptures either due to the cooperative phenomena (direct interaction of closely spaced defects) at modest stress levels or by an unstable propagation of a single macrocrack (brittle failure) at larger stress levels.

The effect of the ruptured bonds on the lattice response in the axial direction can be measured either by the fraction of ruptured diagonals or by the change in the lattice stiffness. The second alternative is strongly preferred since the stiffness can be readily measured on the macro scale and is not size dependent. The size dependence of the response was found to be limited to very small specimens. This conclusion is supported by the test data of Regel' *et al.*, (1974).

The final task focused on the examination of the accuracy of the effective medium estimates of the time to creep rupture, i.e., the effect of the stress concentrations on the failure threshold. The effective medium estimates of the time to rupture was found to be a rather poor upper bound of the exact solution. The poor accuracy of the mean field estimates of the time to creep rupture are attributed to: (a) the assumption that all links must be ruptured prior to the loss of stiffness, and (b) the neglect of the stress concentrations.

The lattice is an exact model of the geometry of resin microstructure which is entirely consistent with its nodular texture (Mijovic and Tsay, 1981, Krajcinovic and Mallick, 1994, 1995). The relative lack of sensitivity to the specimen sizes above 1–2 mm renders this model very appealing for both qualitative and quantitative analyses. Quantitative analysis would require generalization to three dimensions and a detailed study of crosslinking needed for better estimates of the activation energy and link stiffnesses for a given resin. The existence of rather simple analytical estimates, based on the physics of the deformation, is a testimony to the fact that a micromechanical model may often lead to a simpler solution than an empirical or phenomenological artifice.

The simulations reported in this study appear to be similar to those described by Termonia and his collaborators who considered the effect of the molecular weight, strain rate and temperature on strength of polymer fibers formed by an ensemble of fully extended molecular chains. The purely geometrical difference (triangular vs square lattice), dictated by the microstructure itself, was not a reason for this study. The objectives, approach and accomplishments of this study are not identical to those of the studies of Termonia *et al.* The objective of this study was to provide a simple but accurate one parameter analytical model for the creep and creep rupture of a resin specimen subjected to high temperature and relatively modest tensile stresses. This objective was successfully met by determining the only size-independent measure of damage (effective stiffness) which is easily identifiable and measurable in tests. It was also shown that the model can be then formulated in terms of a single parameter (time to rupture). The statistics of this parameter is found to follow the Weibull distribution. Moreover, it was demonstrated that the time to rupture is also size independent which provides the final link between the tests on small specimens and the actual (potentially large) structure. A short discussion of the relative effects of the spatial correlation of defects (stress concentrations) and the topology at failure demonstrates the reason for the failure of effective-medium models which are commonly used in analysis and high temperature design. In summary, it seems that the formulated model provides a foundation for the formulation of a rational design model for the creep failure of resin specimens which can be verified by few simple tests.

Acknowledgements—The authors gratefully acknowledge the financial support in form of a research grant from the U.S. Department of Energy, Office of the Basic Energy Research, Division of Engineering and Geosciences to the Arizona State University which made this work possible.

REFERENCES

Ashby, M. F. (1983) Mechanisms of deformation and fracture. In *Advances in Applied Mechanics*, (eds J. W. Hutchinson and T. Y. Wu) Vol. 23, pp. 117–177. Academic Press Inc., New York, NY.

Ashby, M. F. and Dyson, B. F. (1984) *Creep damage mechanics and micromechanisms*, *Report DMA(A)* 77, Nat. Physics Lab. Teddington, UK.

Beale, P. D. and Srolovitz, D. J. (1988) Elastic fracture in random materials. *Physics Review B* **37**, 5500–5507.

Bolotin, V. V. (1989) *Prediction of Service Life for Machines and Structures*. ASME Press, New York, NY.

Bueche, F. (1955) Tensile strength of plastics above the glass temperature. *Journal of Applied Physics* **26**, 1133–1140.

Cocks, A. C. F. and Leckie, F. A. (1987) Creep continuum equations for damaged materials. In *Advances in Applied Mechanics*, (eds J. W. Hutchinson and T. Y. Wu) Vol. 25, pp. 239–294. Academic Press Inc., New York, NY.

Curtin, W. A. and Scher, H. (1991) Analytic model for scaling of breakdown. *Physics Review Letters* **67,** 2457–2460.
Curtin, W. A. and Scher, H. (1992) Algebraic scaling of materiai strength. *Physics Review B* **45,** 2620–2627.
Dobrodumov, A. V. and El'yashevich, A. M. (1973) Simulation of brittle fracture of polymers by a network model with the Monte Carlo Method. *Soviet Physics Solid State* **15,** 1259–1260.
Duxbury P. M., Kim, S. C. and Leath P. L. (1994) Size effect and statistics of fracture in random materials. *Materials Science Engineering A* **176,** 25–31.
Eyring, H. (1936) Viscosity, plasticity and diffusion as examples of absolute reaction rates. *Journal of Chemical Physics* **4,** 283–291.
Feng, S. and Sen, P. N. (1984) Percolation on elastic networks: new exponent and threshold. *Phyhsics Review Letters* **52,** 216–219.
Hansen, A., Roux, S. and Hinricsen, E. L. (1990) Annealed model for break-down processes'. *Europhyics Letters* **13,** 517–522.
Hansen, A., Roux, S. and Herrmann, H. J. (1989) Rupture of central force lattice. *Journal of Physics France* **50,** 733–744.
Hult, J. A. H. (1966) *Creep in Engineering Structures*, Blaisdell Publ. Co., Waltham, MA.
Hult, J. A. H. (1974) Creep in continua and structures. In *Topics in Applied Mechanics*, (eds J. L. Zeman and F. Ziegler) pp. 137–155. Springer-Verlag, Wien.
Lemieuks, M. A., Breton P. and Trembly, A.-M. S. (1985) Unified approach to numerical transfer matrix methods for disordered systems: application to mixed crystals and to elasticity percolation. *Journal of Physique Letters* **46,** L-1–L-7.
Kachanov, L. M. (1958) On the creep rupture time. *Izv. AN SSSR Otd. Tekhn. Nauk.* **8,** 26–31.
Krajcinovic, D. and Basista, M. (1991) Rupture of central-force lattice revisited'. *J. de Phys. I* **1,** 241–245.
Krajcinovic, D., Lubarda, V. and Sumarac, D. (1993) Some fundamental aspects of the brittle cooperative phenomena—effective continua models. *Mechanics of Materials* **15,** 99–115.
Krajcinovic, D. and Mallick, K. (1994) Creep rupture of polymers. In *Damage Mechanics in Composites*, (eds D. H. Allen and J. W. Ju) ASME Publ., AMD 185, New York, NY.
Krajcinovic, D. and Mallick, K. (1995) Micromechanics of the process induced damage evolution in thermosets. *Journal of Mechanics and Physics of Solids* **43,** 1059–1086.
Krajcinovic, D. and Mastilovic, S. (1995) Some fundamental issues of damage mechanics. *Mech. Mat.* **21,** 217–230.
Krajcinovic, D. and Silva, M. A. G. (1982) Statistical aspects of the continuous damage theory. *International Journal of Solids and Structures* **18,** 551–562.
Krausz, A. S. and Krausz, K. (1988) *Fracture Kinetics of Crack Growth*. Kluwer Academic Publishers, Dordrecht, The Netherlands.
Mijovic, J. and Tsay, L. (1981) Correlations between dynamic mechanical properties and nodular morphology of cured epoxy resins. *Polymer* **20,** 1095–1107.
Meares, P. (1965) *Polymers: Structure and Bulk Properties*. D. Van Nostrand Co. Ltd., New York, NY.
Monette, L. and Anderson, P. M. (1994) Elastic and fracture properties of the two-dimensional triangular and square lattices. *Modelling Simulations of Materials Science Engineering* **2,** 53–66.
Nemat-Nasser, S. and Hori, M. (1993) *Micromechanics: Overall Properties of Heterogeneous Materials*. North-Holland, Amsterdam, The Netherlands.
Perepechko, I. I. (1981) *An Introduction to Polymer Physics*. Mir Publ., Moscow, USSR.
Poirier, J.-P. (1990) *Creep of Crystals*. Cambridge Univ. Press, Cambridge, UK.
Rabotnov, Y. N. (1966) *Creep of Structural Elements*. Nauka Publ., Moscow, USSR.
Raj, R. (1983) Mechanisms of creep-fatigue interaction. In *Flow and Fracture at Elevated Temperatures*, (ed. R. Raj) pp. 121–148. ASM.
Regel', V. R., Slutsker, A. I. and Tomashevskii, E. E. (1974) *The Kinetic Nature of the Strength of Solids*. Nauka Publ., Moscow, USSR.
Riedel, H. (1987) *Fracture at High Temperatures*. Springer-Verlag, Berlin, Germany.
Sahimi, M. and Goddard, J. D. (1986) Elastic percolation models for cohesive mechanical failure in heterogeneous systems. *Physics Review B* **33,** 7848–7851.
Sieradzki, K. and Li, R. (1986) Fracture behavior of a solid with random porosity. *Physics Review Letters* **56,** 2509–2511.
Stauffer, D. and Aharony, A. (1992) *Introduction to Percolation Theory*. Taylor & Francis, London, UK.
Termonia, Y., Meakin, P. and Smith, P. (1985) Theoretical study of the influence of molecular weight on the maximum tensile strength of polymer fibers. *Macromolecules* **18,** 2246–2252.
Termonia, Y. and Smith, P. (1987) Kinetic model for tensile deformation of polymers. 1. Effect of molecular weight. *Macromolecules* **20,** 835–838.
Termonia, Y. and Smith, P. (1988) Kinetic model for tensile deformation of polymers. 2. Effect of entanglement spacing. *Macromolecules* **21** 2184–2189.
Termonia, Y. and Smith, P. (1988) Kinetic model for tensile deformation of polymers. 3. Effect of deformation rate and temperature. *Macromolecules* **21,** 3485–3489.
Termonia, Y. and Walsh, D. J. (1989) Kinetic model for the mechanical properties of polymer glasses. *Journal of Materials Science* **24,** 247–251.
Tobolsky, A. and Eyring, H. (1943) Mechanical properties of polymeric materials. *Journal of Chemical Physics* **11,** 125–134.
Zhurkov, S. N. (1965) Kinetic concept of the strength of solids. *International Journal of Fracture Mechanics* **1,** 311–323.